https://doi.org/10.5194/egusphere-2025-3284
Preprint. Discussion started: 15 July 2025

Contrasting Inland-Coastal Aerosol Mixing States: An Entropy-Based Metric for CCN Activity

Jingye Ren[1,2], Wei Xu[3], Ru-Jin Huang[1*], Fang Zhang[4*], Ying Wang[1], Lu Chen[5], Jurgita Ovadnevaite[6], Darius Ceburnis[6], Colin O'Dowd[6]

[1]*State Key Laboratory of Loess Science, Institute of Earth Environment, Chinese Academy of Sciences, Xi'an, 710061, China,*

[2]*Xi'an Institute for Innovative Earth Environment Research, Xi'an, 710061, China,*

[3]*State Key Laboratory of Advanced Environmental Technology, Institute of Urban Environment, Chinese Academy of Sciences, Xiamen, 361021, China,*

[4]*School of Civil and Environmental Engineering, Harbin Institute of Technology, Shenzhen, 518005, China,*

[5]*School of Ocean and Geographic Science, Yancheng Teachers University, Yancheng 224051, China,*

[6]*School of Natural Sciences, Centre for Climate & Air Pollution Studies, Ryan Institute, University of Galway, University Road, Galway, Ireland*

Corresponding author: Ru-Jin Huang, *rujin.huang@ieecas.cn;* Fang Zhang, *zhangfang2021@hit.edu.cn*

https://doi.org/10.5194/egusphere-2025-3284
Preprint. Discussion started: 15 July 2025

Abstract

Simplified assumptions of aerosol hygroscopic mixing states in modeling studies often introduce substantial uncertainties in estimating cloud condensation nuclei (CCN) concentrations and their climatic impacts. This study systematically investigates the contrasting relationships between mixing states and CCN activity by comparing ambient measurements from inland and coastal sites. We show distinct seasonal variations of the particles mixing state. In winter, externally mixed particles dominated both sites, with comparable mixing state indices (χ) of 0.38±0.12 and 0.39±0.09 respectively for coastal air masses and inland air. However, summer measurements showed pronounced differences: photochemical processes promoted significantly higher internal mixing in coastal aerosols (χ=0.69±0.19), whereas inland χ values only increased moderately to 0.47±0.12. A universal logarithmic correlation was identified between the critical diameter (D_{cri}) characterizing CCN activity and χ (D_{cri} = -32.15ln(χ)+84.71, Pearson r = -0.74), but with distinct decrement rates for coastal vs. inland aerosols. Our further quantitative analysis reveals a 0.1 increase in χ enhanced winter CCN concentrations (N_{CCN}) by 39–65% under typical cloud supersaturations, whereas this effect diminished to ~9% in summer. These results underscore that mixing states exert more pronounced control over N_{CCN} in diverse environments. Our work provides critical constraints for parameterizing fine aerosols CCN activity in climate models, thereby reducing uncertainties in aerosol–climate effect estimations.

https://doi.org/10.5194/egusphere-2025-3284
Preprint. Discussion started: 15 July 2025

1. Introduction

Atmospheric cloud condensation nuclei (CCNs) are complex mixtures of organic and inorganic components. Their chemical and physical properties make quantifying aerosol-cloud interactions challenging (Liu et al., 2018; Rosenfeld et al., 2019; Xu et al., 2022, 2024; Virtanen et al., 2025), introducing uncertainties into climate effect assessments (Charlson et al., 1992; Shrivastava et al., 2017; IPCC, 2021; Manavi et al., 2025; Chen et al., 2022). Accurate climate model predictions of aerosol impacts require understanding aerosol mixing states under different atmospheric conditions and their effects on CCN activity (Ching et al., 2016; Zheng et al., 2021). Current models often oversimplify mixing states by assuming pure internal or external mixing (Winkler, 1973; Zheng et al., 2021; Stevens et al., 2019; Riemer et al., 2019). This is problematic because mixing states directly determine particle hygroscopicity and CCN estimates (Wang et al., 2010; Ren et al., 2018). For example, CCN activity for internal-mixed aerosols rely more on inorganic components, while external mixtures are more sensitive to organic matter (Ren et al., 2018; Bhattu et al., 2015). Such simplifications can lead to significant errors, e.g., Sotiropoulou et al. (2007) found that mixing state assumptions caused two-fold N_{CCN} estimation errors in global models.

Systematic observations across diverse environments are critical because aerosol mixing states exhibit pronounced spatial-temporal variations (Ye et al., 2018; Liu et al., 2025; Hughes et al., 2018). For example, continental and coastal regions present contrasting scenarios (Ramachandran et al., 2016). The continental areas are dominated by anthropogenic emissions, where aerosol aging is driven by industrial and traffic-

https://doi.org/10.5194/egusphere-2025-3284
Preprint. Discussion started: 15 July 2025

related pollutants (Huang et al., 2014; Ren et al., 2023). Particles here undergo progressive internal mixing via photochemical reactions and coagulation, altering their hygroscopic properties (Ervens et al., 2010). While the coastal regions feature dynamic interactions between marine aerosols (e.g., sea salt) and continental pollutants (Schill et al., 2015; Collins et al., 2013; Cheung et al., 2020). Seasonal shifts in air mass sources (e.g., marine vs. continental dominance) create unique mixing state patterns (Xu et al., 2020, 2021a). For instance, summer photochemical processes in coastal areas can enhance internal mixing, while winter often retains more external mixing due to stable atmospheric conditions.

However, the aerosols in continental and coastal regions have distinct climate feedback mechanisms (Bellouin et al., 2019; Pan et al., 2022; Gong et al., 2023). The continental aerosols influence regional cloud formation, while coastal aerosols affect marine boundary layer clouds that are key components of global climate systems (Liu et al., 2018). But the current models lack regional-specific mixing state parameters and usually assume uniform mixing in both environments. This could lead to large uncertainties in predicting CCN concentrations, highlighting the need for site-specific observations.

Recent studies have used the mixing state index (χ) to characterize aerosol heterogeneity (Zheng et al., 2021; Ching et al., 2017; Yuan et al., 2023), but cross-environment comparisons remain limited. By integrating inland and coastal measurements, this study will focus on addressing two key gaps, (1) How continental vs. marine-dominated environments shape aerosol mixing states and CCN activity; (2)

https://doi.org/10.5194/egusphere-2025-3284
Preprint. Discussion started: 15 July 2025

Whether χ-based CCN parameterizations show regional dependencies, providing critical constraints for climate models.

2. Data and Methods

2.1 Field Campaigns

The inland atmospheric measurements were conducted for two periods from 16 November to 6 December and 29 May to 13 June, respectively in urban Beijing, at the Institute of Atmospheric Physics, Chinese Academy of Sciences (IAP, 39.97° N, 116.37° E). This urban site exhibited highly variable aerosol populations dominated by local anthropogenic sources including vehicular, cooking emissions, and residential heating. Coastal measurements were performed at the Mace Head atmospheric research station (MHD, 53.33° N, 9.90° W) from 1 November 2009 to 30 January 2010 and 11 to 31 August 2010, which located on the west coast of Ireland. Aerosol particles here experience alternating influences from polluted continental and clean marine atmospheres. The map of the sites was shown in Figure 1. More details about the campaigns were given in Fan et al. (2020) and Xu et al. (2021a).

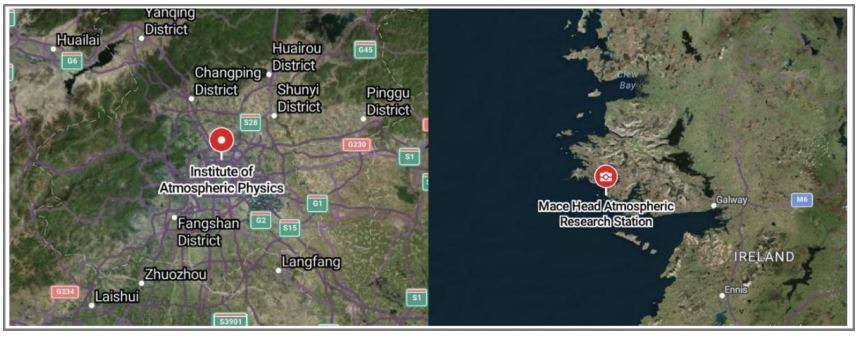

Fig 1. Map of the sites in the Inland of the Institute of Atmospheric Physics (IAP) and

https://doi.org/10.5194/egusphere-2025-3284
Preprint. Discussion started: 15 July 2025

Coastal of Mace Head (MHD). (© Google Maps, https://maps.google.com/, last access: 2 April 2025).

2.2 Instrumentation

Hygroscopicity measurements

The particle hygroscopicity at both sites was characterized using the humidified tandem differential mobility analyzer (HTDMA). The hygroscopic growth factor (Gf), defined as the ratio of the particle diameter at the fixed RH (90%) and dry diameter set in this study for 40, 80, 110, 150, 200 nm at IAP and 35, 50, 75, 110 and 165 nm at MHD, respectively. The Gf probability density function (Gf-PDF) was derived using the TDMAinv algorithm (Gysel et al., 2009).

Here for each particle size, the hygroscopicity parameter κ can be subsequently calculated using κ-Köhler theory (Petters and Kreidenweis, 2007):

$$\kappa = (Gf^3 - 1) \cdot \left[\frac{1}{RH}\exp\left(\frac{4\sigma_s M_w}{RT\rho_w D_d Gf}\right) - 1\right] \quad (1)$$

where RH is the HTDMA relative humidity (90% set in the instrument), $\sigma_{s/a}$ is the surface tension of pure water (0.072 mN m^{-1}), M_w and ρ_w are the molecular weight and the density of pure water, R is the gas constant, and T is the absolute temperature, D_d is the droplet diameter.

Then, the κ-PDF is obtained and normalized as $\int_0^\infty c(\kappa)d\kappa = 1$, where $c(\kappa)$ is normalized as κ-PDF. Further it was used to calculate the particle population heterogeneity (Calculation seen in Section 2.3).

Chemical components

https://doi.org/10.5194/egusphere-2025-3284
Preprint. Discussion started: 15 July 2025

For the inland atmospheric measurements, the non-refractory submicron aerosol (smaller than 1μm, NR-PM_1) chemical composition was quantitatively characterized using the Aerodyne High-Resolution Time-of-Flight Aerosol Mass Spectrometer (HR-ToF-AMS) (DeCarlo et al., 2006), including sulfate (SO_4^{2-}), nitrate (NO_3^-), ammonium (NH_4^+), chloride (ChL) and organics (Org). The black carbon (BC) mass concentration was determined from the light absorption with a seven-wavelength aethalometer (AE33, Magee Scientific Corp.).

Measurements of PM_1 in the coastal atmosphere were also performed by the HR-ToF-AMS, including major inorganic salts (non-sea-salt sulfate, nss-SO_4^{2-}; methanesulfonic acid, MSA; NO_3^-; NH_4^+) and organic matter. The instrument operation and calibration have been described in previous studies (Ovadnevaite et al., 2014; Xu et al., 2019).

Aerosol number size distribution and CCN number concentration

Particle number size distributions (PNSD) were measured using an integrated system consisting of a Differential Mobility Analyzer (DMA; model 3081, TSI Inc.) coupled with a Condensation Particle Counter (CPC; model 3772, TSI Inc.). During the measurements at IAP, the PNSD covered the size range of 10-550 nm with a 5-minute time resolution. It scanned size range of 20-500 nm at MHD with a 10-minute temporal resolution. The CCN number concentrations were quantified at both sites using a Droplet Measurement Technologies CCN counter (DMT-CCNc) (Lance et al., 2006). The instrument's supersaturation (SS) settings were carefully calibrated before and after each campaign using ammonium sulfate aerosol following Rose et al. (2008).

https://doi.org/10.5194/egusphere-2025-3284
Preprint. Discussion started: 15 July 2025

2.3 Calculation the heterogeneity for aerosol particles

To characterize the heterogeneous distribution of the hygroscopic and non-hygroscopic components in populations (Chen et al., 2022), we calculated the mixing state index (χ) using the κ-PDF, following the methodology of Yuan et al. (2023). Two surrogate groups in a population of *N* aerosol particles were assumed (Zheng et al., 2021). One surrogate group consists the non-hygroscopic species with κ_{NH} of 0.01 and another group contains the hygroscopic species with κ_H of 0.6 (Yuan et al., 2023; Ching et al., 2017). At the coastal MHD site, we accounted for the enhanced hydrophilicity of marine aerosols by additionally testing κ_H values of 0.7 and 0.8 (Fig. S1). While these variations in κ_H introduced a mean uncertainty of 8% in χ values, it did not significantly affect the seasonal or site comparisons. The volume fraction of two surrogate groups can be calculated based on the total κ according to the Zdanovskii–Stokes–Robinson (ZSR) mixing rule (Zdanovskii, 1948; Stokes et al., 1966).

The mixing state index χ is defined as the affine ratio of the average particle species diversity (*D*α) and population species diversity (*D*γ) as:

$$\chi = \frac{D_\alpha - 1}{D_\gamma - 1} \quad (2)$$

The average per-particle species diversity *D*α can be calculated as follows. First, the mixing entropies at bin *i* (H_i) are determined according to equation (3),

$$H_i = -P_{i,NH} \times lnP_{i,NH} - P_{i,H} \times lnP_{i,H} \quad (3)$$

where $P_{i,NH}$ and $P_{i,H}$ are the volume fraction of each group for the κ-PDF with X bins at bin *i* (*i*=1,2,…X), and can be determined from the $P_{i,NH} + P_{i,H} = 1$ and $P_{i,NH} \times \kappa_{NH} + P_{i,H} \times \kappa_H = \kappa_i$. Here $\kappa_{NH} = 0.01, \kappa_H = 0.6$; κ_i represents the

https://doi.org/10.5194/egusphere-2025-3284
Preprint. Discussion started: 15 July 2025

hygroscopicity parameter at bin *i*.

Based on the assumption that particles in the same diameter have the same mixing entropy $H_\alpha = \sum_{j=1}^{N} P_j \times H_j$, $P_j = \frac{V_j}{V_{total}} = \frac{1}{N}$; the per-particle mixing entropies H_α is determined according to equation (4),

$$H_\alpha = \sum_{i=1}^{X} H_i \times c(\kappa)_i \times \Delta\kappa \quad (4)$$

where $c(\kappa)_i$ is the probability density of the normalized κ-PDF at bin *i*, and $\Delta\kappa$ represents the bin width. Then, the average per-particle species diversity $D\alpha$ can be determined as $D_\alpha = e^{H_\alpha}$;

The bulk population species diversity $D\gamma$ can be calculated as follows. First, the aerosol population of the mixing entropy can be calculated as equation (5):

$$H_\gamma = -P_{NH} \times lnP_{NH} - P_H \times lnP_H \quad (5)$$

where P_{NH} and P_H are the volume fraction of the non-hygroscopic and hygroscopic components in the population, and can be calculated by equation (6) and (7):

$$P_{NH} = \sum_{i=1}^{X} P_{i,NH} \times c(\kappa)_i \times \Delta\kappa \quad (6)$$

$$P_H = \sum_{i=1}^{X} P_{i,H} \times c(\kappa)_i \times \Delta\kappa \quad (7)$$

Then, the bulk population species diversity $D\gamma$ can be determined as $D_\gamma = e^{H_\gamma}$. Here, the definition of surrogate species as supersets encompassing hygroscopicity heterogeneity implies that the heterogeneity parameter χ ranges from 0 to 1. When the mixing index χ approaches 0, it indicates a completely segregated state where hygroscopic and non-hygroscopic species reside in distinct particles. While for the case the mixing index χ to be 1 represents that the non-hygroscopic and hygroscopic species distributing homogeneously throughout the aerosol population.

https://doi.org/10.5194/egusphere-2025-3284
Preprint. Discussion started: 15 July 2025

3. Result and Discussion

3.1 Comparison of the heterogeneity in the inland and coastal atmosphere

To characterize the hygroscopic heterogeneity of atmospheric aerosols, Figure 2 depicts variations in mixing state metrics (Dα, Dγ, χ) and the hygroscopic parameter (κ_{gf}) across particle size distributions. For inland aerosols, Dα and χ decrease with increasing particle diameter, accompanied by higher κ_{gf} values. This trend indicates that inland particle populations tend to homogenize into hygroscopic compositions through primary particle aging or secondary formation processes (Liu et al., 2025; Chen et al., 2022; Zhong et al., 2022). In contrast, coastal particles exhibit a non-monotonic pattern: Dα and χ decrease for Aitken-mode particles (<100 nm) but increase for accumulation-mode particles. The κ_{gf} shows consistent size-dependent increases in both winter and summer campaigns.

Notably, the mixing state metrics exhibit a pronounced minimum at 75 nm particles, influenced by distinct mechanisms: winter minima reflect the high sea salt fraction, while summer minima are driven by anthropogenic organic matter (Cheung et al., 2020; Xu et al., 2021a). Lower winter χ values—coupled with broader κ-PDF distributions—indicate stronger external mixing and compositional diversity compared to summer (Fig. S2). Seasonal χ and κ_{gf} disparities are more pronounced at the coastal site, primarily driven by the seasonal alternation of marine and anthropogenic emission sources.

https://doi.org/10.5194/egusphere-2025-3284
Preprint. Discussion started: 15 July 2025

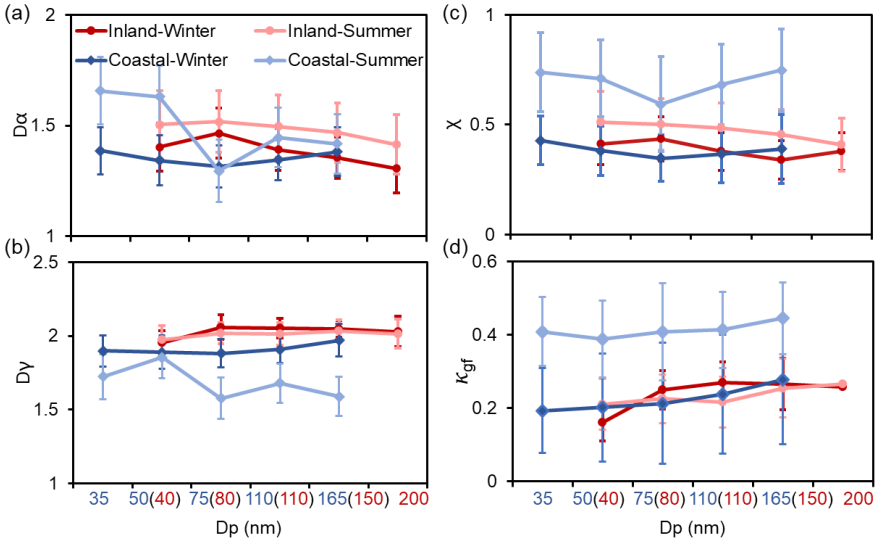

Fig 2. Mean values of the Dα (a), Dγ (b), χ (c) and κ_{gf} (d) for aerosols of five diameters during winter and summer periods in Inland (IAP) and Coastal (Mace Head) sites.

Ultrafine particles (40 nm inland vs. 35 nm coastal, Aitken mode) and larger particles (150 nm inland vs. 165 nm coastal, accumulation mode) were selected to investigate distinct evolutionary processes of aerosol heterogeneity (Fig. 3 and Fig. S3). With the increasing of PM concentration during winter, the variation in χ values exhibit only minor both at the inland and coastal sites, generally fluctuating between approximately −0.04 and 0.08 (Fig. 3a and b). Inland accumulation-mode particles show a modest increase in χ, corresponding with a higher proportion of inorganic salts. Conversely, at coastal sites, the composition fraction shifts from a sea-salt dominance toward organic matter, accompanied by a ~20 % increase in nitrate content (Fig. 3b). In summer, the variation of χ with PM concentration becomes markedly pronounced at both inland and coastal stations. For example, χ for 40 nm particles decreases as PM

https://doi.org/10.5194/egusphere-2025-3284
Preprint. Discussion started: 15 July 2025

increases at inland sites (Fig. 3c). The elevated particle heterogeneity mainly arises from the locally primary emissions and photochemically driven new particle formation. In contrast, χ for 150 nm particles increases from ~0.40 to ~0.60 with rising PM, reflecting enhanced secondary formation and internal mixing during pollution process that render the particle population more homogeneous. At coastal sites, χ declines with rising PM by approximately 0.37 for 35 nm particles and 0.24 for 165 nm particles, mirroring the shift in chemical composition makeup from inorganic dominance to greater organic content (Fig. 3d).

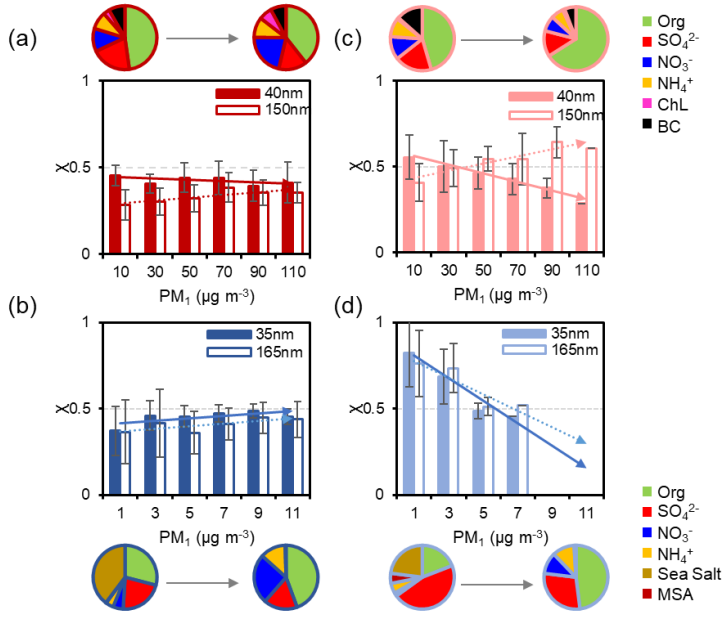

Fig 3. Variation of the average χ of 40 nm and 150 nm in inland and 35 nm and 165 nm in coastal site with the particle mass concentration in Inland-winter (a), Inland-summer (b), Coastal-winter (c) and Coastal-summer (d). The pie charts represent the average mass fraction during four field campaigns.

https://doi.org/10.5194/egusphere-2025-3284
Preprint. Discussion started: 15 July 2025

Figure 4 illustrates pronounced diurnal variations in mixing state metrics (Dα, Dγ, Gf-PDF, χ) between inland and coastal atmospheres. In the inland atmosphere, winter exhibited steeper declines in Dα and χ during evening rush hours than summer, indicating a higher fraction of non-hygroscopic particles (40 nm) from fresh traffic emissions (Fig. 4a1). Concurrently, reduced Dγ values suggest that the bulk population consists of uniformly distributed less-hygroscopic (LH) components (Fig. 4c1). Aitken mode particles showed bimodal and broader Gf-PDF distributions, corresponding to cooking activities (11:00–13:00 LT) and traffic peaks (17:00–20:00 LT) (Cai et al., 2020). Midday photochemical aging promoted more internally mixed aerosols (Yang et al., 2012; Liu et al., 2025), as evidenced by increasing Dα at the urban site (Fig. 4b1). Conversely, accumulation-mode particles showed minimal diurnal variations, suggesting stable relative proportions of LH and more-hygroscopic (MH) components in inland aerosols across seasons.

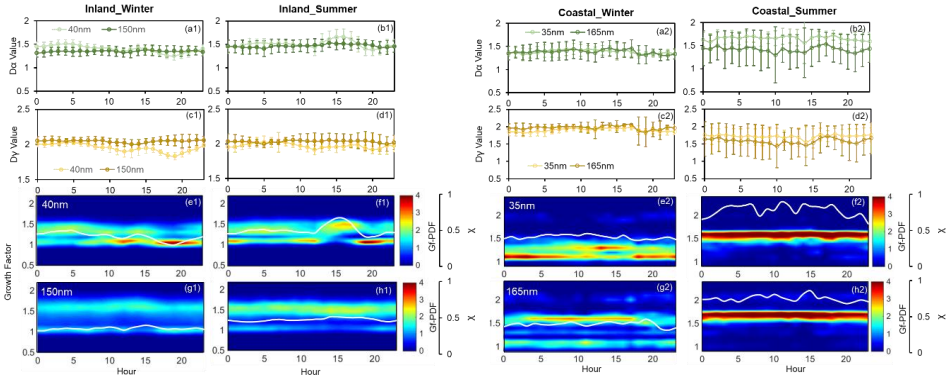

Fig 4. The variation of Dα, Dγ, Gf-PDF, and χ during winter and summer periods for 40 nm and 150 nm aerosols in Inland (a1-h1) and for 35 nm and 165 nm aerosols Coastal site (a2-h2).

https://doi.org/10.5194/egusphere-2025-3284
Preprint. Discussion started: 15 July 2025

For the coastal atmosphere, the mixing state metrics (Dα, Dγ, and χ) of Aitken and accumulation mode particles in winter exhibited analogous diurnal patterns, characterized by a descending trend at nightfall. This corresponds to an enhanced modal distribution of near-hydrophobic (NH) particles at 35 nm and more-hygroscopic (MH) particles at 165 nm. In summer, Dα and Dγ both trended downward during daytime, with the decline of Dγ being more pronounced. A conspicuous seasonal discrepancy between Aitken and accumulation mode particles was observed in this region (Fig. 4a2–h2), where the mixing state index χ increased incrementally from winter to summer. Specifically, the mean χ for 35 nm particles escalated from 0.42 to 0.80, and for 165 nm particles, it rose from 0.39 to 0.76. This trend demonstrates a strong alignment with the spread factor documented by Xu et al. (2021a, b).

The Gf-PDF diurnal profiles of Aitken mode particles displayed a bimodal and broadened distribution, corresponding to a less-hygroscopic (LH) mode of biogenic origin during nighttime and a more-hygroscopic (MH) mode dominated by sea salt (comprising 55% number fraction) during daytime. Analogously, accumulation mode particles exhibited bimodal distributions with a higher proportion of MH mode during daytime, primarily attributed to the prevalence of sea salt and non-sea-salt sulfate (nss-sulfate) in the coastal atmosphere (Xu et al., 2020). In contrast, summer observations revealed that Gf-PDFs of both Aitken and accumulation mode particles transitioned to unimodal distributions, signifying more homogeneous mixing of LH and MH components within individual particles. This uniformity is linked to processes including sulfuric acid condensation, admixture of sulfate with biogenic organic matter (Xu et al.,

https://doi.org/10.5194/egusphere-2025-3284
Preprint. Discussion started: 15 July 2025

2021a), as well as photochemical oxidation and atmospheric aging (Jimenez et al., 2009).

3.2 Dependence of the aerosol properties on the mixing state

The mixing state of particle populations undergoes dynamic transformations during atmospheric aging, profoundly influencing their CCN activity. Unlike prior studies that assumed mixing states based on chemical component fractions (Yang et al., 2012; Padró et al., 2012; Ren et al., 2018), this work employs the entropy-derived mixing state index χ, which quantifies the distribution of hygroscopic and non-hygroscopic species (Zheng et al., 2021; Ching et al., 2017). We systematically investigate how aerosol properties evolve with changing χ. Figure 5 illustrates the dependency of aerosol characteristics on χ (ranging from 0 to 1 in 0.1 increments), presenting key insights into particle size and chemical composition—two fundamental determinants of CCN activity (Ren et al., 2018).

As χ increases, the peak diameter (D_{peak}) of the particle number size distribution (PNSD) shifts toward larger sizes (Fig. 5a and Fig. S4), while peak concentrations occur within the intermediate χ range (0.3–0.6). This trend indicates that CN number concentration (N_{CN}) first increases, driven by primary emissions and new particle formation, then decreases due to mixing and aging processes (Fig. 5b). Notably, inland summer N_{CN} exhibits a sustained slight increase, linked to frequent new particle formation events and subsequent particle growth.

The critical diameter (D_{cri})—defined as the minimum size for activation at a given

https://doi.org/10.5194/egusphere-2025-3284
Preprint. Discussion started: 15 July 2025

298 supersaturation—depends on the mass fraction of soluble components (Petters and
299 Kreidenweis, 2007). Using a typical cloud supersaturation of 0.2% as a case study, Fig.
300 5c shows that D_{cri} decreases with increasing soluble species (e.g., sulfate, nitrate) in the
301 inland atmosphere. In contrast, coastal D_{cri} exhibits nonlinear variations with χ: high
302 external mixing (low χ) elevates D_{cri} due to dominant organic components, reducing sea
303 salt particle fractions. As χ increases, the mass fraction of non-sea-salt sulfate (nss-
304 sulfate) rises, enhancing activation potential by decreasing D_{cri}.

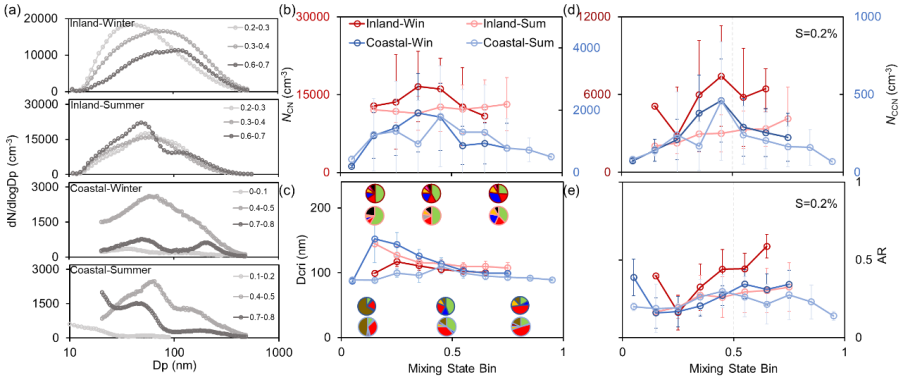

305

306 **Fig 5.** Variation of the average particle number size distribution (PNSD) with the
307 mixing state index χ (a), variation of the N_{CN} with the χ (b), variation of the D_{cri} and
308 mass fraction of chemical composition with the χ (c), variation of the N_{CCN} and
309 activation ratio (AR) at S=0.2% with the χ (d-e).

310 The dependence of CCN activity at 0.2% supersaturation on mixing state index χ
311 reveals distinct inter-atmospheric differences, as shown in Fig. 5d-e. In the inland
312 atmosphere, N_{CCN} at S=0.2% demonstrates a monotonic increasing trend with χ,
313 attributed to the synergistic effects of rising N_{CN} and decreasing D_{cri} (Fig. S5). By
314 contrast, coastal N_{CCN} follows a pattern analogous to N_{CN}, with peak concentrations

https://doi.org/10.5194/egusphere-2025-3284
Preprint. Discussion started: 15 July 2025

shifting toward higher χ values. This highlights the dominant role of particle size effects in enhancing CCN concentrations under marine-influenced conditions (Perkins et al., 2022).

Two distinct D_{cri}-χ trends underpin these disparities: one remains stable, driven by the inherent hygroscopicity of sea salt, while the other exhibits steep D_{cri} declines associated with anthropogenic pollution as internal mixing intensifies. These discrepancies are further manifested in the nonlinear D_{cri}-χ relationship. The activation ratio (AR)—quantifying aerosol cloud droplet formation potential at fixed supersaturation—also varies by site (Fig. 5e). Notably, inland winter AR shows a marked increase with χ, likely due to enhanced N_{CCN} from the elevated inorganic fraction under higher mixing states (Fig. 3). Conversely, the inorganic fraction decreases during other sampling periods, dampening AR growth.

3.3 Impact of the mixing state on the CCN activity

To better interpret the impact of mixing state on CCN concentrations, Fig. 6 quantifies the relative change in N_{CCN} at S=0.2% as mixing state index χ increases, contextualizing how CN concentration and chemical compositions (i.e., D_{cri}) evolve with mixing and aging across particle populations. D_{cri} demonstrates heightened sensitivity to minor χ fluctuations at low mixing states ($\chi < 0.5$; Fig. 6a), whereas further increases in internal mixing (higher χ) exert negligible influence on D_{cri} for already internally mixed particles. This behavior suggests that the D_{cri}-χ relationship may enable a novel parameterization for D_{cri} estimation, a framework that is not yet reported

https://doi.org/10.5194/egusphere-2025-3284
Preprint. Discussion started: 15 July 2025

in prior literature.

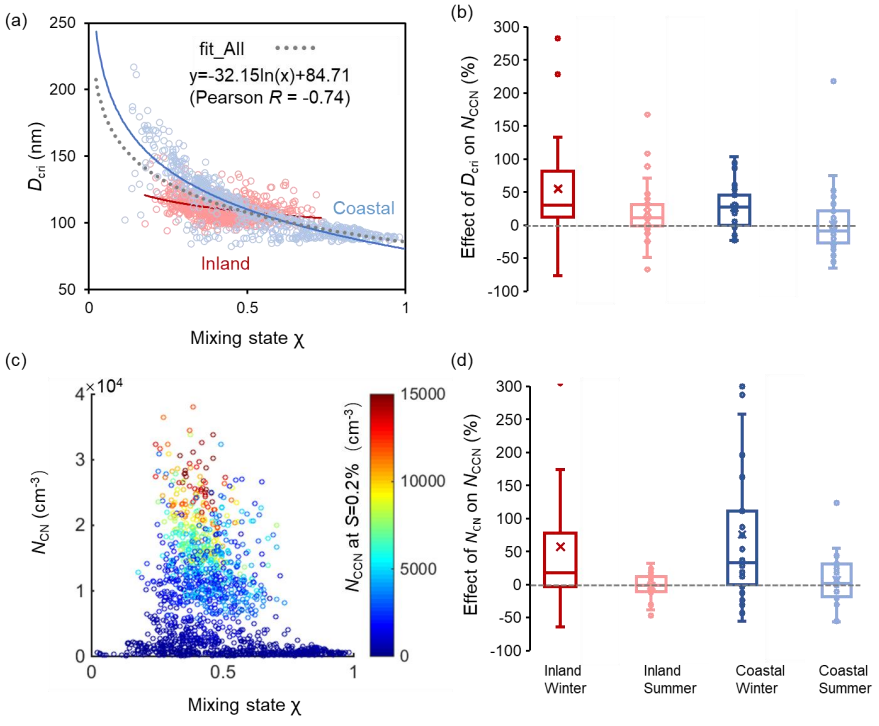

Fig 6. Dependency of the critical diameter (D_{cri}) on the χ (a), relative change of CCN number concentration (N_{CCN}) at supersaturation S = 0.2% with the reduction in D_{cri} (b); Dependency of the CN number concentration (N_{CN}) on the χ, different colors represent the N_{CCN} (c), relative change of N_{CCN} with the change in N_{CN} (d).

Coastal aerosol data points (blue dots) span a broad D_{cri} range (80–220 nm) with χ varying from 0.1 to 1, reflecting alternating influences of highly hygroscopic inorganic salts (sea salt, sulfate) and less-hygroscopic organic matter. In contrast, inland aerosols—dominated by anthropogenic pollutants—exhibit a narrower D_{cri} range (90–150 nm). Both environments show negative D_{cri}-χ correlations, but with distinct functional forms: coastal aerosols feature an exceptional logarithmic fit (D_{cri} = -

https://doi.org/10.5194/egusphere-2025-3284
Preprint. Discussion started: 15 July 2025

42.98ln(χ) +80.36, R^2 = 0.75; Fig. 6a blue line), while inland aerosols (red line) yield a shallower slope (-12.04). Pooling all data, we derive a generalized parameterization: D_{cri} = -32.15ln(χ) + 84.71 (Pearson r = -0.74, R^2 = 0.54).

Box plot analyses (Fig. S6) show mixing state reduces D_{cri} by 2.2–6.8% across campaigns, with the steepest winter decline. χ impacts on N_{CN} differ starkly between environments: positive effects in polluted inland air (+9%) versus negative effects in coastal regions (-2%). Inland aerosols, frequently perturbed by primary emissions and new particle formation, exhibit elevated N_{CN} (peaking at χ = 0.2–0.7), while coastal N_{CN} remains ~5000 cm^{-3} across all χ.

To isolate the impacts of critical diameter (D_{cri}) and condensation nuclei number concentration (N_{CN}) on CCN activity, we categorized data into two groups: C1 (particles within specific N_{CN} ranges) evaluates N_{CCN} variations driven by D_{cri}-χ relationships, while C2 (particles within fixed D_{cri} intervals) assesses N_{CN}-χ effects (Fig. 6b). Relative changes (RC) in D_{cri}, N_{CN}, and N_{CCN} with χ were calculated by comparing successive χ increments (χi+1 vs. χi, i=0,0.1…1) within defined N_{CN}/D_{cri} windows.

Notably, χ exerts more pronounced effects on N_{CCN} for externally mixed aerosols. For example, coastal winter aerosols (high external mixing; χ_{mean}=0.38±0.12) showed N_{CCN} RCs of 23% (C1) and 72% (C2), whereas coastal summer aerosols (high internal mixing; χ_{mean}=0.69±0.19) exhibited negligible effects (-2.5% in C1, 0.9% in C2). Inland atmospheres, despite smaller seasonal χ variations, showed analogous trends: winter N_{CCN} RCs (55% in C1, 57% in C2 for external mixing) exceeded summer values for more internally mixed populations (Fig. 6d). These results confirm that hygroscopic

https://doi.org/10.5194/egusphere-2025-3284
Preprint. Discussion started: 15 July 2025

heterogeneity strongly influences N_{CCN} under external mixing, aligning with prior work (Ching et al., 2017).

Mixing state impacts on N_{CCN} are most pronounced during winter in both environments, attributed to heightened winter D_{cri} sensitivity to χ: a 0.1 χ increase reduces D_{cri} by 5.2% (winter), boosting N_{CCN} by 39%, versus 2.4% D_{cri} reduction (summer) yielding only 6% N_{CCN} enhancement. Concomitantly, winter N_{CN}-χ effects on N_{CCN} reach 65%, far exceeding summer responses.

Contrasting with prior evaluation methods that oversimplify mixing states (Ren et al., 2018; Xu et al., 2021b), the entropy-based framework adopted herein enables explicit quantification of CCN activity evolution in response to mixing state transitions. Inland winter aerosols are presumably shaped by intense urban pollution sources—including traffic emissions, residential heating, and cooking activities—thereby enriching the externally mixed particle fraction (Fan et al., 2020; Xie et al., 2020). Analogously, coastal winter aerosols exhibit dominant external mixing, consisting of near-hydrophobic and hydrophilic particle mixtures (Xu et al., 2021a). As illustrated in Fig. S2, winter aerosol populations display bimodal or multimodal κ–PDF distributions, evidencing high-degree external mixing with chemically diverse compositions. These results collectively highlight the pivotal role of mixing state heterogeneity in modulating CCN activity across environments.

4. Conclusions

The mixing state of aerosol populations undergoes complex transformations during atmospheric aging, altering the distribution of hygroscopic and non-hygroscopic

https://doi.org/10.5194/egusphere-2025-3284
Preprint. Discussion started: 15 July 2025

components and thus influencing CCN activity (Xu et al., 2021a; Ching et al., 2017). This study derived a mixing state index from field-measured hygroscopicity probability density functions, systematically investigating its impacts on CCN activity in inland and coastal environments. Results provide field evidence that aerosol mixing states generally reside between purely internal and external extremes (Chen et al., 2022), highlighting a dual regulatory mechanism of mixing state on CCN activity. As χ increases, CN number concentrations (N_{CN}) first rise—driven by primary emissions and new particle formation—then decline due to condensation and coagulation during aging. Additionally, a logarithmic decreasing relationship between critical diameter (D_{cri}) and χ was identified for both inland and coastal particles, parameterized as $D_{cri} = -32.15\ln(\chi) + 84.71$ (Pearson $R = -0.74$, $R^2 = 0.54$). This offers a practical approach to estimate D_{cri} from χ, serving as a general framework for integrating mixing state effects on CCN activity in atmospheric models.

Entropy-based analyses confirm the pivotal role of mixing state in regulating N_{CCN}, especially for externally mixed aerosols: a 0.1 χ increase can enhance N_{CCN} by 39–65%. Current models often oversimplify aerosol mixing states as purely internal or external (Stevens et al., 2019; Bauer et al., 2013), the latter being particularly sensitive to organic matter (Ren et al., 2018; Bhattu et al., 2015). Such simplifications introduce significant biases in N_{CCN} estimation (Riemer et al., 2019; Ching et al., 2019). The χ-D_{cri} parameterization proposed here offers a novel approach to reduce model complexity in representing aerosol hygroscopicity and CCN activation, enabling more accurate simulations of aerosol CCN capacity. This advancement improves our understanding of

https://doi.org/10.5194/egusphere-2025-3284
Preprint. Discussion started: 15 July 2025

aerosol-cloud interactions (IPCC, 2021; Rosenfeld et al., 2019), critical for refining climate effect assessments.

Data availability

All data used in the study are available at https://doi.org/10.3974/geodb.2019.06.11.V1 (Fan et al., 2019) and http://doi.org/10.17632/3dx6pnx869.1 (Xu et al., 2021a).

Author contributions

RH and JR conceived the conceptual development of the paper. JR, FZ and WX directed and performed the experiments with YW and LC. FZ provided the dataset in the inland site. JO, DC and CO provided the dataset in the coastal site. JR conducted the data analysis and wrote the draft. All authors edited and commented on the various sections of the paper.

Competing interests

The contact author has declared that none of the authors has any competing interests.

Supporting Information

Additional analysis results that were applied in this study. Sensitivity of the hygroscopic parameter for the group of the hygroscopic species on the mixing state index χ (Figure S1), mean values of the κ–PDF for aerosols of five diameters (Figure S2), time series of the average per-particle species diversity $D\alpha$, the bulk population species diversity $D\gamma$, and their affine ratio χ (Figure S3), variation of the peak diameter (D_{peak}) with the mixing state index (Figure S4), diurnal variation of χ and CN

https://doi.org/10.5194/egusphere-2025-3284
Preprint. Discussion started: 15 July 2025

concentration during winter and summer periods for 40 nm and 150 nm aerosols in inland and for 35 nm and 165 nm aerosols in coastal site (Figure S5), relative change of the critical diameter and CN concentration with the mixing state index χ (Figure S6) (PDF).

Acknowledgements

This work was funded by the National Natural Science Foundation of China (NSFC) under Grant No. 42525301, 42405118 and 42475112, the State Key Laboratory of Loess Science, Institute of Earth Environment, Chinese Academy of Sciences (SKLLQG2429), the Guangdong Natural Science Foundation (Grant No. 2024A1515011005). We thank all participants of the field campaign for their hard work and sharing of the data.

References

Bhattu, D., Tripathi, S. N.: CCN closure study: Effects of aerosol chemical composition and mixing state, Journal of Geophysical Research: Atmospheres., 120(2), 766-783, https://doi.org/10.1002/2014JD021978, 2015.

Bellouin, N., Quaas, J., Gryspeerdt, E., Kinne, S., Stier, P.,Watson-Parris, D., Boucher, O., Carslaw, K. S., Christensen, M., Daniau, A.-L., Dufresne, J.-L., Feingold, G., Fiedler, S., Forster, P., Gettelman, A., Haywood, J. M., Lohmann, U., Malavelle, F., Mauritsen, T., McCoy, D. T., Myhre, G., Mülmenstädt, J., Neubauer, D., Possner, A., Rugenstein, M., Sato, Y., Schulz, M., Schwartz, S. E., Sourdeval, O., Storelvmo, T., Toll, V., Winker, D., Stevens, B.: Bounding global aerosol radiative forcing of climate change, Rev. Geophys., 58, e2019RG000660, https://doi.org/, 2019.

Bauer, S. E., Ault, A., Prather, K. A.: Evaluation of aerosol mixing state classes in the

https://doi.org/10.5194/egusphere-2025-3284
Preprint. Discussion started: 15 July 2025

458 GISS modelE-MATRIX climate model using single-particle mass spectrometry
459 measurements, Journal of Geophysical Research: Atmospheres., 118, 9834-9844,
460 https://doi.org/10.1002/jgrd.50700, 2013.
461 Chen, Y., Haywood, J., Wang, Y., Malavelle, F., Jordan, G., Partridge, D., Fieldsend, J.,
462 Leeuw, J. D., Schmidt, A., Cho, N., Oreopoulos, L., Platnick, S., Grosvenor, D.,
463 Field, P., Lohmann, U.: Machine learning reveals climate forcing from aerosols is
464 dominated by increased cloud cover, Nature Geoscience., 15(8), 609-614,
465 https://doi.org/10.1038/s41561-022-01027-9, 2022.
466 Chen, A., Zhao, C., Zhang, H., Yang, Y., Li, J.: Surface albedo regulates aerosol direct
467 climate effect, Nature Communications., 15(1), 7816, https://doi.org/
468 10.1038/s41467-024-52255-z, 2024.
469 Charlson, R. J., Schwartz, S. E., Hales, J. M., Cess, R. D., Coakley Jr, J. A., Hansen, J.
470 E., Hofmann, D. J.: Climate forcing by anthropogenic aerosols, Science.,
471 255(5043), 423-430, https://doi.org/10.1126/science.255.5043.423, 1992.
472 Ching, J., Zaveri, R. A., Easter, R. C., Riemer, N., Fast, J. D.: A three-dimensional
473 sectional representation of aerosol mixing state for simulating optical properties
474 and cloud condensation nuclei, Journal of Geophysical Research: Atmospheres.,
475 121(10), 5912-5929, https://doi.org/10.1002/2015JD024323, 2016.
476 Collins, D. B., Ault, A. P., Moffet, R. C., Ruppel, M. J., Cuadra-Rodriguez, L. A.,
477 Guasco, T. L., Corrigan, C. E., Pedler, B. E., Azam, F., Aluwihare, L. I., Bertram,
478 T. H., Roberts, G. C., Grassian, V. H., Prather, K. A.: Impact of marine
479 biogeochemistry on the chemical mixing state and cloud forming ability of nascent
480 sea spray aerosol, Journal of Geophysical Research: Atmospheres., 118(15), 8553-
481 8565, https://doi.org/10.1002/jgrd.50598, 2013.
482 Cheung, H. C., Chou, C. C. K., Lee, C. S. L., Kuo, W. C., Chang, S. C.: Hygroscopic
483 properties and cloud condensation nuclei activity of atmospheric aerosols under
484 the influences of Asian continental outflow and new particle formation at a coastal
485 site in eastern Asia, Atmospheric Chemistry and Physics., 20(10), 5911-5922,
486 https://doi.org/10.5194/acp-20-5911-2020, 2020.

https://doi.org/10.5194/egusphere-2025-3284
Preprint. Discussion started: 15 July 2025

Chen, L., Zhang, F., Zhang, D., Wang, X., Song, W., Liu, J., Ren, J., Jiang, S., Li, X., and Li, Z.: Measurement report: Hygroscopic growth of ambient fine particles measured at five sites in China, Atmospheric Chemistry and Physics., 22, 6773-6786, https://doi.org/10.5194/acp-22-6773-2022, 2022.

Cai, J., Chu, B., Yao, L., Yan, C., Heikkinen, L. M., Zheng, F., Li, C., Fan, X., Zhang, S., Yang, D., Wang, Y., Kokkonen, T. V., Chan, T., Zhou, Y., Dada, L., Liu, Y., He, H., Paasonen, P., Kujansuu, J. T., Petäjä, T., Mohr, C., Kangasluoma, J., Bianchi, F., Sun, Y., Croteau, P. L., Worsnop, D. R., Kerminen, V. M., Du, W., Kulmala, M., & Daellenbach, K. R.: Size-segregated particle number and mass concentrations from different emission sources in urban Beijing, Atmospheric Chemistry and Physics., 20(21), 12721-12740, https://doi.org/10.5194/acp-20-12721-2020, 2020.

Cai, M., Tan, H., Chan, C. K., Qin, Y., Xu, H., Li, F., Schurman, M. I., Liu, L., Zhao, J.: The size-resolved cloud condensation nuclei (CCN) activity and its prediction based on aerosol hygroscopicity and composition in the Pearl Delta River (PRD) region during wintertime 2014, Atmospheric Chemistry and Physics., 18(22), 16419-16437, https://doi.org/10.5194/acp-18-16419-2018, 2018.

Ching, J., Fast, J., West, M., Riemer, N.: Metrics to quantify the importance of mixing state for CCN activity, Atmospheric Chemistry and Physics., 17(12), 7445-7458, https://doi.org/10.5194/acp-17-7445-2017, 2017.

Ching, J., Adachi, K., Zaizen, Y., Igarashi, Y., Kajino, M.: Aerosol mixing state revealed by transmission electron microscopy pertaining to cloud formation and human airway deposition, npj Climate and Atmospheric Science., 2(1), 22, https://doi.org/10.1038/s41612-019-0081-9, 2019.

DeCarlo, P. F., Kimmel, J. R., Trimborn, A., Northway, M. J., Jayne, J. T., Aiken, A. C., Gonin, M., Fuhrer, K., Horvath, T., Docherty, K. S., Worsnop, D. R., Jimenez, J. L.: Field-deployable, high-resolution, time of-flight aerosol mass spectrometer, Analytical Chemistry., 78, 8281-8289, https://doi.org/10.1021/ac061249n, 2006.

Ervens, B., Cubison, M. J., Andrews, E., Feingold, G., Ogren, J. A., Jimenez, J. L., Quinn, P. K., Bates, T. S., Wang, J., Zhang, Q., Coe, H., Flynn, M., Allan, J. D.:

https://doi.org/10.5194/egusphere-2025-3284
Preprint. Discussion started: 15 July 2025

CCN predictions using simplified assumptions of organic aerosol composition and mixing state: a synthesis from six different locations, Atmospheric Chemistry and Physics., 10(10), 4795-4807, https://doi.org/10.5194/acp-10-4795-2010, 2010.

Fan, X., Liu, J., Zhang, F., Chen, L., Collins, D., Xu, W., Jin, X., Ren, J., Wang, Y., Wu, H., Li, S., Sun, Y., Li, Z.: Contrasting size-resolved hygroscopicity of fine particles derived by HTDMA and HR-ToF-AMS measurements between summer and winter in Beijing: the impacts of aerosol aging and local emissions, Atmospheric Chemistry and Physics., 20(2), 915-929, https://doi.org/10.5194/acp-20-915-2020, 2020.

Gong, X., Zhang, J., Croft, B., Yang, X., Frey, M. M., Bergner, N., Chang, R. Y. W., Creamean, J. M., Kuang, C., Martin, R. V., Ranjithkumar, A., Sedlacek, A. J., Uin, J., Willmes, S., Zawadowicz, M. A., Pierce, J. R., Shupe, M. D., Schmale, J., Wang, J.: Arctic warming by abundant fine sea salt aerosols from blowing snow, Nature Geoscience., 16(9), 768-774, https://doi.org/10.1038/s41561-023-01254-8, 2023.

Gysel, M., Mcfiggans, G. B., Coe, H.: Inversion of tandem differential mobility analyser (TDMA) measurements, Journal of Aerosol Science., 40(2), 134-151, https://doi.org/10.1016/j.jaerosci.2008.07.013, 2009.

Hughes, M., Kodros, J. K., Pierce, J. R., West, M., Riemer, N.: Machine learning to predict the global distribution of aerosol mixing state metrics, Atmosphere., 9(1), 15, https://doi.org/10.3390/atmos9010015, 2018.

Huang, R. J., Zhang, Y., Bozzetti, C., Ho, K. F., Cao, J. J., Han, Y., Daellenbach, K. R., Slowik, J. G., Platt, S. M., Canonaco, F., Zotter, P., Wolf, R., Pieber, S. M., Bruns, E. A., Crippa, M., Ciarelli, G., Piazzalunga, A., Schwikowski, M., Abbaszade, G., Schnelle-Kreis, J., Zimmermann, R., An, Z., Szidat, S., Baltensperger, U., Haddad, I. E., Prévôt, A. S.: High secondary aerosol contribution to particulate pollution during haze events in China, Nature., 514(7521), 218-222, https://doi.org/10.1038/nature13774, 2014.

IPCC. Summary for Policymakers. In Climate Change 2021: The Physical Science Basis. Contribution of Working Group I to the Sixth Assessment Report of the

https://doi.org/10.5194/egusphere-2025-3284
Preprint. Discussion started: 15 July 2025

Intergovernmental Panel on Climate Change; Cambridge University Press: Cambridge, United Kingdom and New York, NY, USA, 2021.

Jimenez, J. L., Canagaratna, M. R., Donahue, N. M., Prevot, A. S. H., Zhang, Q., Kroll, J. H., DeCarlo, P. F., Allan, J. D., Coe, H., Ng, N. L., Aiken, A. C., Docherty, K. S., Ulbrich, I. M., Grieshop, A. P., Robinson, A. L., Duplissy, J., Smith, J. D., Wilson, K. R., Lanz, V. A., Hueglin, C., Sun, Y., Tian, J., Laaksonen, A., Raatikainen, T., Rautiainen, J., Vaattovaara, P., Ehn, M., Kulmala, M., Tomlinson, J. M., Collins, D. R., Cubison, M. J., Dunlea, E. J., Huffman, J. A., Onasch, T. B., Alfarra, M. R., Williams, P. I., Bower, K., Kondo, Y., Schneider, J., Drewnick, F., Borrmann, S., Weimer, S., Demerjian, K., Salcedo, D., Cottrell, L., Griffin, R., Takami, A., Miyoshi, T., Hatakeyama, S., Shimono, A., Sun, J., Zhang, Y., Dzepina, K., Kimmel, J. R., Sueper, D., Jayne, J. T., Herndon, S. C., Trimborn, A. M., Williams, L. R., Wood, E. C., Middlebrook, A. M., Kolb, C. E., Baltensperger, U., Worsnop, D. R.: Evolution of organic aerosols in the atmosphere, Science., 326(5959), 1525-1529, https://doi.org/10.1126/science.1180353, 2009.

Liu, J., Zhang, F., Ren, J., Chen, L., Zhang, A., Wang, Z., Zou, S., Xu, H., Yue, X.: The evolution of aerosol mixing state derived from a field campaign in Beijing: implications for particle aging timescales in urban atmospheres, Atmospheric Chemistry and Physics., 25(9), 5075-5086, https://doi.org/10.5194/acp-25-5075-2025, 2025.

Liu, P., Song, M., Zhao, T., Gunthe, S. S., Ham, S., He, Y., Qin, Y., Gong, Z., Amorim, C. J., Bertram, K. A., Martin, S. T.: Resolving the mechanisms of hygroscopic growth and cloud condensation nuclei activity for organic particulate matter, Nature communications., 9(1), 4076, https://doi.org/10.1038/s41467-018-06622-2, 2018.

Lance, S., Nenes, A., Medina, J., Smith, J. N.: Mapping the operation of the DMT continuous flow CCN counter, Aerosol Science and Technology., 40(4), 242-254, https://doi.org/10.1080/02786820500543290, 2006.

Manavi, S. E. I., Aktypis, A., Siouti, E., Skyllakou, K., Myriokefalitakis, S., Kanakidou,

https://doi.org/10.5194/egusphere-2025-3284
Preprint. Discussion started: 15 July 2025

M., Pandis, S. N.: Atmospheric aerosol spatial variability: Impacts on air quality and climate change, One Earth., 8(3), https://doi.org/10.1016/j.oneear.2025.101237, 2025.

Ovadnevaite, J., Ceburnis, D., Leinert, S., Dall'Osto, M., Canagaratna, M., O'Doherty, S., Berresheim, H., O'Dowd, C.: Submicron NE Atlantic marine aerosol chemical composition and abundance: Seasonal trends and air mass categorization, Journal of Geophysical Research: Atmospheres., 119, 11850-11863, https://doi.org/10.1002/2013JD021330, 2014.

Pan, Z., Mao, F., Rosenfeld, D., Zhu, Y., Zang, L., Lu, X., Thornton, J. A., Holzworth, R. H., Yin, J., Efraim, A., Gong, W.: Coarse Sea spray inhibits lightning, Nature Communications., 13(1), 4289, https://doi.org/10.1038/s41467-022-31714-5, 2022.

Petters, M. D., Kreidenweis, S. M.: A single parameter representation of hygroscopic growth and cloud condensation nucleus activity, Atmospheric Chemistry and Physics., 7(8), 1961-1971, https://doi.org/10.5194/acp-7-1961-2007, 2007.

Padró, L. T., Moore, R. H., Zhang, X., Rastogi, N., Weber, R. J., and Nenes, A.: Mixing state and compositional effects on CCN activity and droplet growth kinetics of size-resolved CCN in an urban environment, Atmospheric Chemistry and Physics., 2012, 12, 10239-10255, https://doi.org/10.5194/acp-12-10239-2012, 2012.

Perkins, R. J., Marinescu, P. J., Levin, E. J. T., Collins, D. R., Kreidenweis, S. M.: Long- and short-term temporal variability in cloud condensation nuclei spectra over a wide supersaturation range in the Southern Great Plains site, Atmospheric Chemistry and Physics., 22(9), 6197-6215, https://doi.org/10.5194/acp-22-6197-2022, 2022.

Rosenfeld, D., Zhu, Y., Wang, M., Zheng, Y., Goren, T., Yu, S.: Aerosol- driven droplet concentrations dominate coverage and water of oceanic low-level clouds, Science., 363(6427), https://doi.org/10.1126/science. aay4194, 2019.

https://doi.org/10.5194/egusphere-2025-3284
Preprint. Discussion started: 15 July 2025

Riemer, N., Ault, A. P., West, M., Craig, R. L., Curtis, J. H.: Aerosol mixing state: Measurements, modeling, and impacts, Reviews of Geophysics., 57(2), 187-249, https://doi.org/10.1029/2018RG000615, 2019.

Ren, J., Zhang, F., Wang, Y., Collins, D., Fan, X., Jin, X., Xu, W., Sun, Y., Cribb, M., Li, Z.: Using different assumptions of aerosol mixing state and chemical composition to predict CCN concentrations based on field measurements in urban Beijing, Atmospheric Chemistry and Physics., 18(9), 6907-6921, https://doi.org/10.5194/acp-18-6907-2018 2018.

Ramachandran, S., Srivastava, R.: Mixing states of aerosols over four environmentally distinct atmospheric regimes in Asia: coastal, urban, and industrial locations influenced by dust, Environmental Science and Pollution Research., 23, 11109-11128, https://doi.org/10.1007/s11356-016-6254-8, 2016.

Ren, J., Zhang, F., Chen, L., Cao, G., Liu, M., Li, X., Wu, H., Cheng, Y., and Li, Z.: Identifying the hygroscopic properties of fine aerosol particles from diverse sources in urban atmosphere and the applicability in prediction of cloud nuclei, Atmos. Environ., 298, 119615, https://doi.org/10.1016/j.atmosenv.2023.119615, 2023.

Rose, D., Gunthe, S. S., Mikhailov, E., Frank, G. P., Dusek, U., Andreae, M. O., Pöschl, U.: Calibration and measurement uncertainties of a continuous-flow cloud condensation nuclei counter (DMT-CCNC): CCN activation of ammonium sulfate and sodium chloride aerosol particles in theory and experiment, Atmospheric Chemistry and Physics., 8(5), 1153-1179, https://doi.org/10.5194/acp-8-1153-2008, 2008.

Shrivastava, M., Cappa, C. D., Fan, J., Goldstein, A. H., Guenther, A. B., Jimenez, J. L., Kuang, C., Laskin, A., Martin, S. T., Ng, N. L., Petaja, T., Pierce, J. R., Rasch, P. J., Roldin, P., Seinfeld, J. H., Shilling, J., Smith, J. N., Thornton, J. A., Volkamer, R., Wang, J., Worsnop, D. R., Zaveri, R. A., Zelenyuk, A., Zhang, Q.: Recent advances in understanding secondary organic aerosol: Implications for global climate forcing, Reviews of Geophysics., 55(2), 509-559,

https://doi.org/10.5194/egusphere-2025-3284
Preprint. Discussion started: 15 July 2025

https://doi.org/10.1002/2016RG000540, 2017.

Stevens, R., and Dastoor, A.: A Review of the Representation of Aerosol Mixing State in Atmospheric Models, Atmosphere., 10, 168, https://doi.org/10.3390/atmos10040168, 2019.

Sotiropoulou, R. E. P., Nenes, A., Adams, P. J., Seinfeld, J. H.: Cloud condensation nuclei prediction error from application of Köhler theory: Importance for the aerosol indirect effect, Journal of Geophysical Research: Atmospheres., 112(D12), https://doi.org/10.1029/2006JD007834, 2007.

Schill, S. R., Collins, D. B., Lee, C., Morris, H. S., Novak, G. A., Prather, K. A., Quinn, P. K., Sultana, C. M., Tivanski, A. V., Zimmermann, K., Cappa, C. D., Bertram, T. H.: The impact of aerosol particle mixing state on the hygroscopicity of sea spray aerosol, ACS central science., 1(3), 132-141, https://doi.org/10.1021/acscentsci.5b00174, 2015.

Stokes, R. H., Robinson, R. A.: Interactions in aqueous nonelectrolyte solutions. I. Solute-Solvent equilibria, Journal of Physical Chemistry., 70(7), 2126-2130, https://doi.org/10.1021/j100879a010, 1966.

Virtanen, A., Joutsensaari, J., Kokkola, H., Partridge, G. D., Blichner, S., Seland, Ø., Holopainen, E., Tovazzi, E., Lipponen, A., Mikkonen, S., Leskinen, A., Hyvärinen, A., Zieger, P., Krejci, R., Ekman, A. M. L., Riipinen, I., Quaas, J., Romakkaniemi, S.: High sensitivity of cloud formation to aerosol changes, Nature Geoscience., 1-7, https://doi.org/10.1038/s41561-025-01662-y, 2025.

Winkler, P.: The growth of atmospheric aerosol particles as a function of the relative humidity—II. An improved concept of mixed nuclei, Journal of Aerosol Science., 4(5), 373–387, https://doi.org/10.1016/0021-8502(73)90027-X, 1973.

Wang, J., Cubison, M. J., Aiken, A. C., Jimenez, J. L., Collins, D. R.: The importance of aerosol mixing state and size-resolved composition on CCN concentration and the variation of the importance with atmospheric aging of aerosols, Atmospheric Chemistry and Physics., 10(15), 7267-7283, https://doi.org/10.5194/acp-10-7267-2010, 2010.

https://doi.org/10.5194/egusphere-2025-3284
Preprint. Discussion started: 15 July 2025

659 Xu, W., Ovadnevaite, J., Fossum, K. N., Lin, C., Huang, R.-J., O'Dowd, C., Ceburnis,
660 D.: Seasonal trends of aerosol hygroscopicity and mixing state in clean marine and
661 polluted continental air masses over the Northeast Atlantic, Journal of Geophysical
662 Research: Atmospheres., 126, e2020JD033851,
663 https://doi.org/10.1029/2020JD033851, 2021a.
664 Xu, W., Fossum, K. N., Ovadnevaite, J., Lin, C., Huang, R. J., O'Dowd, C., Ceburnis,
665 D.: The impact of aerosol size-dependent hygroscopicity and mixing state on the
666 cloud condensation nuclei potential over the north-east Atlantic, Atmospheric
667 Chemistry and Physics., 21(11), 8655-8675, https://doi.org/10.5194/acp-21-8655-
668 2021, 2021b.
669 Xu, W., Ovadnevaite, J., Fossum, K. N., Lin, C., Huang, R. J., O'Dowd, C., Ceburnis,
670 D.: Aerosol hygroscopicity and its link to chemical composition in the coastal
671 atmosphere of Mace Head: marine and continental air masses, Atmospheric
672 Chemistry and Physics., 20(6), 3777-3791, https://doi.org/10.5194/acp-20-3777-
673 2020, 2020.
674 Xu, W., Sun, Y., Wang, Q., Zhao, J., Wang, J., Ge, X., Xie, C., Zhou, W., Du, W., Li, J.,
675 Fu, P., Wang, Z., Worsnop, D. R., Coe, H.: Changes in aerosol chemistry from
676 2014 to 2016 in winter in Beijing: Insights from high-resolution aerosol mass
677 spectrometry, Journal of Geophysical Research: Atmospheres., 124, 1132-1147,
678 https://doi.org/10.1029/2018JD029245, 2019.
679 Xu, W., Ovadnevaite, J., Fossum, K. N., Lin, C., Huang, R. J., Ceburnis, D., O'Dowd,
680 C.: Sea spray as an obscured source for marine cloud nuclei, Nature Geoscience.,
681 15(4), 282-286, https://doi.org/10.1038/s41561-022-00917-2, 2022.
682 Xu, W., Ovadnevaite, J., Fossum, K. N., Huang, R. J., Huang, D., Zhong, H., Gu, Y.,
683 Lin, C., Huang, C., O'Dowd, C., Ceburnis, D.: Condensation of organic-inorganic
684 vapours governs the production of ultrafine secondary marine cloud nuclei,
685 Communications Earth & Environment., 5(1), 359,
686 https://doi.org/10.1038/s43247-024-01519-z, 2024.
687 Xie, C., He, Y., Lei, L., Zhou, W., Liu, J., Wang, Q., Xu, W., Qiu, Y., Zhao, J., Sun, J.,

https://doi.org/10.5194/egusphere-2025-3284
Preprint. Discussion started: 15 July 2025

Li, L., Li, M., Zhou, Z., Fu, P., Wang, Z., Sun, Y.: Contrasting mixing state of black carbon-containing particles in summer and winter in Beijing, Environmental Pollution., 263, 114455, https://doi.org/10.1016/j.envpol.2020.114455, 2020.

Ye, Q., Gu, P., Li, H. Z., Robinson, E. S., Lipsky, E. M., Kaltsonoudis, C., Lee, A. K. Y., Apte, J. S., Robinson, A. L., Sullivan, R. C., Presto, A. A., Donahue, N. M.: Spatial variability of sources and mixing state of atmospheric particles in a metropolitan area, Environmental Science & Technology., 52, 6807-6815, https://doi.org/10.1021/acs.est.8b01011, 2018.

Yuan, L., and Zhao, C.: Quantifying particle-to-particle heterogeneity in aerosol hygroscopicity, Atmospheric Chemistry and Physics., 23, 3195-3205, https://doi.org/10.5194/acp-23-3195-2023, 2023.

Yang, F., Chen, H., Du, J., Yang, X., Gao, S., Chen, J., Geng, F.: Evolution of the mixing state of fine aerosols during haze events in Shanghai, Atmospheric Research., 104: 193-201, https://doi.org/10.1016/j.atmosres.2011.10.005, 2012.

Zheng, Z., West, M., Zhao, L., Ma, P.-L., Liu, X., and Riemer, N.: Quantifying the structural uncertainty of the aerosol mixing state representation in a modal model, Atmospheric Chemistry and Physics., 21, 17727–17741, https://doi.org/10.5194/acp-21-17727-2021 , 2021.

Zheng, Z., Curtis, J. H., Yao, Y., Gasparik, J. T., Anantharaj, V. G., Zhao, L., West, M., Riemer, N.: Estimating submicron aerosol mixing state at the global scale with machine learning and Earth system modeling, Earth and Space Science., 8(2), e2020EA001500, https://doi.org/10.1029/2020EA001500, 2021.

Zdanovskii, A.: New methods for calculating solubilities of electrolytes in multicomponent systems, Zh. Fiz. Khim. C, 22, 1475–1485, 1948.

Zhong, H., Huang, R. J., Lin, C., Xu, W., Duan, J., Gu, Y., Huang, W., Ni, H.; Zhu, C., You, Y., Wu, Y., Zhang, R., Ovadnevaite, J., Ceburnis, D., O'Dowd, C.: Measurement report: On the contribution of long-distance transport to the secondary aerosol formation and aging, Atmospheric Chemistry and Physics., 22, 9513-9524, https://doi.org/10.5194/acp-22-9513-2022, 2022.